A shadow of the repulsive Rutherford scattering in the laboratory frame

Žugec, Petar; Rudec, Dario

OPEN ACCESS
IOP Publishing
European Journal of Physics
Eur. J. Phys. **42** (2021) 055018 (18pp)
https://doi.org/10.1088/1361-6404/ac172d

A shadow of the repulsive Rutherford scattering in the laboratory frame

Petar Žugec* **and Dario Rudec**

Department of Physics, Faculty of Science, University of Zagreb, Zagreb, Croatia

E-mail: pzugec@phy.hr

Received 24 December 2020, revised 8 July 2021
Accepted for publication 22 July 2021
Published 10 August 2021

Abstract

The paper explores the Rutherford scattering shadow in an entire class of comoving frames—inertial frames moving along the initial projectile direction—of which the laboratory frame, where the target is initially at rest, is a representative example. The paper is a continuation of the previous work addressing the scattering shadow in the fixed-target and the center-of-mass frame. It is shown that the transition from these frames is technically quite involved, due to the scattering shadow forming at an infinite distance from an initial target position. The central procedure involves solving the 5th degree polynomial as a part of an associated extremization procedure. The shadow existence itself is subject to certain conditions, dependent on a given comoving frame. A new and unexpected phenomenon is found within a certain set of comoving frames, including the laboratory frame itself. It consists of a phase transition between an entirely smooth type of shadow and the one characterized by a formation of a sharp edge.

Keywords: Rutherford scattering, shadow, comoving frame, laboratory frame

Supplementary material for this article is available online

1. Introduction

The famous historical experiments by Geiger and Marsden [1–3], dealing with the scattering of α-particles by thin metal foils, are appropriately considered not only as the turning points in physics, but also as the turning points of a rare kind in the development of the modern civilization. These experiments have, in a most direct manner and for the first time in a history of mankind, allowed Rutherford to reveal the inner structure of the atom [4], thus discovering the existence of the atomic nucleus and ushering the age of nuclear technology. Aside from the obvious social benefits of having discovered a novel and usable source of energy, these

*Author to whom any correspondence should be addressed.

0143-0807/21/055018+18$33.00

achievements have inadvertently had an unprecedented influence upon our understanding of the entire universe—from a very start of its existence (the primordial nucleosynthesis) to the origin of life on Earth (the stellar nucleosynthesis from the Sun, as a source of all life-sustaining energy on Earth).

In a recent work [5] a remarkable feature of this scattering—nowadays known as the Rutherford scattering and understood to be the scattering the electric charges due to the Coulomb interaction—was analyzed in some detail. This feature consist in the repulsive Rutherford scattering casting a proverbial shadow, shielding (under appropriately defined conditions) an entire portion of space from admitting any charged particle trajectory. The form of this shadow was first investigated in the fixed-target frame and the center-of-mass frame, and was shown to be paraboloidal in both frames. Though the Rutherford scattering itself is a regular subject of (under)graduate physics courses, as a very cornerstone of nuclear physics, and though its shadowing effect is at the center of a material surface investigation method known as low-energy ion scattering spectroscopy [6, 7], the shadowing feature seems to be little known throughout the educational literature. And all this despite it being fully within the mathematical capabilities of any (under)graduate student in physical sciences. The latest attempt at rekindling the interest in this worthy educational subject has already attracted attention and has lead to further illuminating expositions [8, 9]. We have high hopes that all these efforts will lead to a widespread recognition of this topic's deserved place in physical studies.

There have been earlier isolated attempts at drawing attention to the Rutherford scattering shadow [10–13], mostly limited to the fixed-target frame—an accelerated frame of the charged target itself, where the target is at rest at all times. One of the earliest such references, by Adolph *et al* [10], comments upon the particle trajectories in the laboratory frame—an inertial frame where the charged target is at rest only at the initial moment—stating that '*the construction of the orbits* (in the laboratory frame) *is beyond the reach of simple geometry*'. We will obtain these trajectories by a Galilean transformation of the trajectories from the fixed-target frame. Even more generally, we will analyze it within an entire class of comoving frames, consisting of any inertial frame moving in an appropriate direction, with the constant speed relative to the center-of-mass frame, i.e. to the particle-target system as a whole.

We adopt here a classical nonrelativistic approach. We hope to demonstrate that many, to our knowledge new results may yet be gained within this approach. We will show that, as far as the Rutherford scattering shadow is concerned, the transition between the frames in relative motion is not just a technical challenge from which no further insight could be gained. Quite the contrary: in opposition to the naive idea that the scattering shadow in the comoving frame might be obtained by some simple manipulation of the parabolic shadow from the fixed-target frame, we will find that: (1) several technical challenges appear, consisting of a divergent integral and the 5th degree polynomial; (2) the resulting shadow is no longer parabolic; (3) the scattering shadow cannot form in just any inertial frame; (4) there appears a qualitative alteration in the shadow behavior, akin to a certain type of phase transition, consisting in a formation of a sharp edge along the shadow caustic.

We face some instructive challenges in the derivation of the projectile trajectories (restricted to appendix A). The first challenge is the appearance of a divergent integral, that we overcome by a careful and disciplined parametrization of the emerging divergence. The second challenge is the necessity for finding numerical solutions to the 5th degree polynomial, since there exists no solution in radicals for a general polynomial of a degree greater than 4. There is a certain educational benefit in the ability to demonstrate the practical utilization of the modern computer resources in solving a particular, very well defined physical problem, appropriate even at lower levels of the (under)graduate studies where the Rutherford scattering is a regular subject.

Returning to the issue of the nonrelativistic approach, there is a rich discussion to be had, carried out in section 2. In section 3 we illustrate the procedure for obtaining the projectile trajectories in the comoving frame. The technical derivation is presented in appendix A. In section 4 a procedure for obtaining the scattering shadow from these trajectories is presented. Section 5 addresses and identifies the necessary conditions for the existence of the scattering shadow. Section 6 focuses on the laboratory frame, as one of the most prominent examples of comoving frames. Section 7 summarizes the main conclusions of this work.

This paper is accompanied by the supplementary note (http://stacks.iop.org/EJP/42/055018/mmedia), expanding upon the main material presented herein. We stress that this paper is self-contained and that addressing the supplementary note is by no means necessary for following the main content. Still, the supplementary note offers deep, exciting and—to our knowledge—many novel expositions of various aspects of the repulsive Rutherford scattering in the comoving frame, to be appreciated by an interested reader.

2. The (non)relativistic treatment

In the laboratory frame the charged target is put into motion by the recoil, which leads both to the transformation of its electric field and the additional induction of the magnetic field. The electric field transforms not only due to the target's non-zero speed, but also obtains a radiative component due to the target's acceleration. This is clearly seen from a well known, relativistically correct expression for the electric field of an arbitrarily moving point charge [14, 15]:

$$\mathbf{E}(\mathbf{r},t)=\frac{q}{4\pi\epsilon_0}\left[\frac{\hat{\mathbf{n}}-\boldsymbol{\beta}}{\gamma^2K^3R^2}+\frac{\hat{\mathbf{n}}\times((\hat{\mathbf{n}}-\boldsymbol{\beta})\times\mathbf{a})}{c^2K^3R}\right]_\tau, \tag{1}$$

where q is the value of the charge and ϵ_0 is the vacuum permittivity. With $\mathbf{R}$ as a position-vector of a point at which the field is to be calculated ($\mathbf{r}$) relative to the position of the point charge ($\mathbf{r}'$): $\mathbf{R}=\mathbf{r}-\mathbf{r}'=R\,\hat{\mathbf{n}}$, the terms R and $\hat{\mathbf{n}}$ appearing in (1) are its norm and unit direction, respectively: $R=|\mathbf{R}|$ and $\hat{\mathbf{n}}=\mathbf{R}/R$. Alongside $\mathbf{v}=\mathrm{d}\mathbf{r}'/\mathrm{d}t$ as the velocity of the point charge, $\mathbf{a}=\mathrm{d}\mathbf{v}/\mathrm{d}t$ as its acceleration and c as the speed of light in vacuum, $\boldsymbol{\beta}=\mathbf{v}/c$ is the standard relativistic notation, together with the Lorentz factor $\gamma=(1-\boldsymbol{\beta}\cdot\boldsymbol{\beta})^{-1/2}$ and $K=1-\hat{\mathbf{n}}\cdot\boldsymbol{\beta}$. Finally, $[\cdot]_\tau$ denotes that all quantities within the square brackets are to be calculated at the retarded time τ such that $\tau+R(\tau)/c=t$, since it takes finite time for the information to propagate from $\mathbf{r}'$ to $\mathbf{r}$. It is to be noted that the first term in square brackets ($\propto 1/R^2$) is the field transformation solely due the motion of the charge, while the second one ($\propto 1/R$) is the radiative component due to its acceleration. This separation of contributions to the electric field due to the 'levels' of motion is even more clearly seen from an equivalent Feynman's formula [16]:

$$\mathbf{E}(\mathbf{r},t)=\frac{q}{4\pi\epsilon_0}\left(\left[\frac{\hat{\mathbf{n}}}{R^2}\right]_\tau+\frac{[R]_\tau}{c}\frac{\mathrm{d}}{\mathrm{d}t}\left[\frac{\hat{\mathbf{n}}}{R}\right]_\tau+\frac{1}{c^2}\frac{\mathrm{d}^2[\hat{\mathbf{n}}]_\tau}{\mathrm{d}t^2}\right), \tag{2}$$

where the first term is evidently the pure Coulomb field (electrostatic in form), the second term takes into account the general motion of the charge, while only the third term may produce the dependence upon the charge acceleration. The associated magnetic field of the point charge may be calculated from its electric field as:

$$\mathbf{B}(\mathbf{r},t)=\frac{\left[\hat{\mathbf{n}}\right]_\tau\times\mathbf{E}(\mathbf{r},t)}{c}. \tag{3}$$

It is worth noting that in case of the charge moving with the constant velocity, (3) may also be expressed as:

$$\mathbf{B}_{\mathbf{a}=\mathbf{0}} = \frac{\boldsymbol{\beta} \times \mathbf{E}_{\mathbf{a}=\mathbf{0}}}{c}. \tag{4}$$

This is easily seen since applying the vector products from either relation leaves only $\boldsymbol{\beta} \times \hat{\mathbf{n}}$ in place of the first term from (1). In fact, the relation from (4) holds not only for the point charge, but for any charge distribution moving with the constant velocity [17].

If we were to calculate the scattering trajectories by solving the relativistic equations of motion in the laboratory (or any other inertial) frame, we would simply use the correct field expressions (1) and (3), properly taking into account all aspects of the field transformations (the departure from the electrostatic form, the induction of the magnetic field and the appearance of the radiative component). However, would we have to account for these effects if we treated the problem nonrelativistically, staying within the confines of Galilean mechanics? This can be judged based on the relative magnitude between the electric and magnetic forces in a given frame. In the nonrelativistic case any effect from the charge acceleration upon the electric field from (1) is suppressed by $1/c^2$, thus being negligible. In the absence of this term the magnetic field may be expressed as in (4), meaning that for the nonrelativistic charge it always holds $\mathbf{B} \approx \mathbf{v} \times \mathbf{E}/c^2$. Now it is simple enough to inspect the relative magnitude between the forces exerted upon the charged projectile (p) by the charged target (t):

$$\frac{F_{\mathbf{B}}}{F_{\mathbf{E}}} = \frac{|q_{\mathrm{p}}\mathbf{v}_{\mathrm{p}} \times \mathbf{B}_{\mathrm{t}}|}{|q_{\mathrm{p}}\mathbf{E}_{\mathrm{t}}|} \propto \frac{v_{\mathrm{p}} v_{\mathrm{t}}}{c^2}. \tag{5}$$

Thus, in the nonrelativistic limit ($v_{\mathrm{p}}, v_{\mathrm{t}} \ll c$) the Lorentz force is negligible, relative to an electric one, fully justifying the Galilean treatment that we adopt in this work.

Once the nonrelativistic treatment has been justified and adopted based on (5), the Lorentz force must not be taken into account (assuming that the magnetic field appears due to the transformation of the electric field between the frames in relative motion). The reason is the Galilean invariance of force, combined with the fact that—within the Galilean framework—the electric field retains the electrostatic form $\mathbf{E}(\mathbf{r}, t) = (q/4\pi\epsilon_0)\hat{\mathbf{n}}/R^2$ in all frames, which is easily seen from the nonrelativistic limit of (1). The short argument is this. Consider the electrostatic force exerted upon the point charge q: $\mathbf{F} = q\mathbf{E}$. When the transition is made to a frame moving with the relative velocity $\mathbf{v}$, the force is furnished by an additional, Lorentz component: $\mathbf{F}' = q\mathbf{E}' + q\mathbf{v} \times \mathbf{B}'$. However, from the demonstrated nonrelativistic invariance of the electrostatic field ($\mathbf{E} = \mathbf{E}'$) and the Galilean invariance of force ($\mathbf{F} = \mathbf{F}'$) it follows that $q\mathbf{v} \times \mathbf{B}' = \mathbf{0}$, i.e. there is no room left for any kind of effect by the magnetic field.

The previous argument is closely related to one of the two independent Galilean limits to the classical electrodynamics [18–20], the so-called electric limit wherein the electric effects are dominant ($|\mathbf{E}| \gg c|\mathbf{B}|$). It was formally shown in a famous paper by Le Bellac and Lévy-Leblond [18] that if the Galilean invariance is to be preserved in the electric limit, one must indeed contend with the magnetic field exerting no force upon the electric charge, rather than taking any kind of low-velocity limit of the electric field that would account for the necessity of an additional, Lorentz force ($q\mathbf{v} \times \mathbf{B}' \neq \mathbf{0}$ due to $\mathbf{E} \neq \mathbf{E}'$). However, this argument is not strictly applicable to our case, since the Galilean limits to the classical electrodynamics apply to the inertial frames in relative motion. We, on the other hand, will be concerned with the transition between the accelerated (fixed-target) frame and the inertial (comoving) frame.

Related to the approach that we adopt in this work—boosting the charged particle trajectories from the fixed-target into the comoving frame by means of a Galilean transformation—let

us suppose for a moment that we attempted to perform this procedure relativistically. If we managed to obtain the relativistic particle trajectories in the fixed-target frame, we would have to perform the relativistic boost into the comoving frame by employing the generalized Lorentz transformations for the noninertial frames [21]. Although the correct field transformations between the frames would be implicitly accounted for by thus transformed trajectories, it would make little sense attempting to perform a relativistic boost of the classical hyperbolic trajectories—as they are not the relativistic solutions themselves—unless one were to use them as the reasonable approximations to the fully relativistic trajectories in the fixed-target frame.

3. Coulomb trajectories in the comoving frame

We will obtain the charged particle trajectories in the comoving frame by a Galilean boost of well known hyperbolic trajectories from the fixed-target frame. We remind the reader of the basic steps leading to these hyperbolic solutions. With projectile and target charges Z_p and Z_t, respectively, in units of the elementary charge e, and ϵ_0 as the vacuum permittivity, one starts from a Coulomb force $\mathbf{F}_{\mathrm{t}\to\mathrm{p}}$ exerted upon the charged projectile:

$$\mathbf{F}_{\mathrm{t}\to\mathrm{p}} = \frac{Z_\mathrm{p} Z_\mathrm{t} e^2}{4\pi\epsilon_0} \frac{\mathbf{r}_\mathrm{p} - \mathbf{r}_\mathrm{t}}{|\mathbf{r}_\mathrm{p} - \mathbf{r}_\mathrm{t}|^3}, \tag{6}$$

and performs a standard separation of variables by introducing the target-relative projectile position[1] $\mathbf{r} \equiv \mathbf{r}_\mathrm{p} - \mathbf{r}_\mathrm{t}$ and the center-of-mass position $\mathbf{R} \equiv (m_\mathrm{p}\mathbf{r}_\mathrm{p} + m_\mathrm{t}\mathbf{r}_\mathrm{t})/(m_\mathrm{p} + m_\mathrm{t})$. In doing so the motion of the system as a whole ($\mathbf{R}$) decouples from the relative motion ($\mathbf{r}$). The equation of the relative motion then reads:

$$\ddot{\mathbf{r}} = \frac{Z_\mathrm{p} Z_\mathrm{t} e^2}{4\pi\epsilon_0 \mu} \frac{\mathbf{r}}{r^3}, \tag{7}$$

where the reduced mass μ of a projectile-target system appears, determined by the projectile and target masses m_p and m_t as $\mu^{-1} \equiv m_\mathrm{p}^{-1} + m_\mathrm{t}^{-1}$. With the appropriate set of initial conditions expressed in cylindrical coordinates:

$$\mathbf{r}(t=0) = \varrho_0 \hat{\boldsymbol{\rho}} - \left(\lim_{z_0 \to \infty} z_0 \right) \hat{\mathbf{z}}, \tag{8}$$

$$\dot{\mathbf{r}}(t=0) = v_0 \hat{\mathbf{z}}, \tag{9}$$

the solution for the radial component of the target-relative projectile position $\mathbf{r}$ reduces to:

$$r(\theta) = \frac{\varrho_0^2}{2\left(\varrho_0 \tan\frac{\theta}{2} - \chi\right)\cos^2\frac{\theta}{2}}, \tag{10}$$

with this particular form being the most convenient to this work. The polar angle θ is a conventionally defined spherical coordinate relative to the z-axis oriented along the projectile's initial

[1] Our term for the 'fixed-target frame' comes from a definition of a relative position $\mathbf{r}$: in a frame where we can equate the projectile position with $\mathbf{r}$, the target is by construction at rest, fixed at the origin of the frame. Therefore, the 'fixed-target' term should not be confused with target being infinitively massive or held in place by an external force. For a finitely massive target the fixed-target frame is accelerated, as the target is continuously being recoiled from the incoming projectile. An alternative, somewhat mouthful term to be found in literature for this frame is the 'instantaneous rest frame (of the charge)'.

velocity. An impact parameter ϱ_0 determines a specific projectile trajectory and corresponds to the initial distance from the z-axis. The central parameter χ is defined as:

$$\chi \equiv \frac{Z_\mathrm{p} Z_\mathrm{t} e^2}{4\pi\epsilon_0 \mu v_0^2}, \tag{11}$$

with v_0 as the initial relative speed between the target and projectile, that remains invariant under Galilean transformations. The infinity from the z-component of the initial relative position (8) will propagate into later calculations, therefore we need to carefully parameterize so as to formally keep it under control. In this work we choose to parameterize it by a positive parameter z_0.

In the absence of external forces a center-of-mass position $\mathbf{R}$ satisfies the equation of motion $\ddot{\mathbf{R}} = \mathbf{0}$, meaning that the system as a whole cannot accelerate spontaneously. In other words, the total linear momentum of the isolated system is conserved. Immediately introducing the shorthands:

$$\eta_\mathrm{p,t} \equiv \frac{m_\mathrm{p,t}}{m_\mathrm{p} + m_\mathrm{t}}, \tag{12}$$

the definitions of $\mathbf{r}$ and $\mathbf{R}$ may be inverted in order to recover the absolute projectile and target coordinates in any reference frame:

$$\mathbf{r}_\mathrm{p} = \mathbf{R} + \eta_\mathrm{t}\mathbf{r}, \tag{13}$$

$$\mathbf{r}_\mathrm{t} = \mathbf{R} - \eta_\mathrm{p}\mathbf{r}, \tag{14}$$

where the motion of the frame itself—or, equivalently, of the entire physical system within the given frame—is reflected solely through $\mathbf{R}$. Given the initial center-of-mass position $\mathbf{R}_0$, the solution to $\ddot{\mathbf{R}} = \mathbf{0}$ is a rectilinear motion with the constant velocity $\mathbf{V}_\mathrm{cm}$:

$$\mathbf{R}(t) = \mathbf{R}_0 + \mathbf{V}_\mathrm{cm} t. \tag{15}$$

Among all possible inertial frames, we limit our attention only to those moving along the z-axis ($\mathbf{V}_\mathrm{cm} = V_\mathrm{cm}\hat{\mathbf{z}}$), corresponding to the projectile's initial direction of motion. In addition, the origin of the coordinate frame will coincide with the target's initial position. Specifically, the final solution in the laboratory frame—where the target is at rest at the initial moment, so that $\dot{r}_\mathrm{t}^{(\mathrm{lab})}(t=0) = \mathbf{0}$ and $\dot{r}_\mathrm{p}^{(\mathrm{lab})}(t=0) = v_0\hat{\mathbf{z}}$—may always be recovered from the general solution by taking $V_\mathrm{cm}^{(\mathrm{lab})} = \eta_\mathrm{p} v_0$.

In order to specify that the target is initially at the origin of the comoving frame, we complement the initial relative position (8) by a consistent set of initial absolute positions:

$$\mathbf{r}_\mathrm{p}(t=0) = \varrho_0\hat{\boldsymbol{\rho}} - \left(\lim_{z_0\to\infty} z_0\right)\hat{\mathbf{z}}, \tag{16}$$

$$\mathbf{r}_\mathrm{t}(t=0) = \mathbf{0}. \tag{17}$$

From a definition of the center-of-mass position it now trivially follows that: $\mathbf{R}_0 = \eta_\mathrm{p}\mathbf{r}_\mathrm{p}(t=0)$.

Though compelling due to several interesting technical changeless, the derivation of the Coulomb trajectories in the comoving frame is rather tedious and results in somewhat lengthy expressions. However, it is of central importance to this work so we present it in appendix A (instead of the supplementary note). For conciseness we only sketch here the general procedure and present the final results.

- Starting from the known projectile trajectories (10) in the fixed-target frame, use the non-relativistic kinematics from (13) and (14) in order to obtain a Galilean boost into the comoving frame.
- In performing a Galilean transformation, a divergent integral appears; carefully parameterize this divergence by means of a well defined limit:

$$\mathcal{Z}_0 = \left(\frac{V_{\rm cm}}{v_0} - \eta_{\rm p}\right) \lim_{z_0\to\infty} z_0 + \frac{V_{\rm cm}}{v_0}\chi \lim_{z_0\to\infty} \ln \frac{2z_0}{{\rm e}\mathcal{L}}, \tag{18}$$

  in order to isolate it from the relevant part of expression. In that, an arbitrary length scale $\mathcal{L}$ appears, formally required for an argument of the logarithm to be dimensionless. A natural logarithm base e also appears here, not to be confused with the unit charge e.
- Separate the parameterized divergence from the z-component $z_{\rm p}$ of the particle trajectory such that:

$$z_{\rm p} = \mathcal{Z}_{\rm p} + \mathcal{Z}_0, \tag{19}$$

  which is equivalent to the shift in coordinate origin by $\mathcal{Z}_0$, and continue calculations with the remaining, finite part of the expression:

$$\begin{aligned}\mathcal{Z}_{\rm p}(\rho_{\rm p}) = {}& \frac{V_{\rm cm}}{v_0}\chi\left(\frac{\rho_{\rm p}}{\eta_{\rm t}\varrho_0} + \ln\frac{\mathcal{L}(\rho_{\rm p}-\varrho_0)}{\eta_{\rm t}\chi\varrho_0} - \frac{\eta_{\rm p}}{\eta_{\rm t}}\right)\\ &+ \left(\frac{V_{\rm cm}}{\eta_{\rm t}v_0}+1\right)\left(\frac{\varrho_0(\rho_{\rm p}-\varrho_0)}{2\chi} - \frac{\chi(\rho_{\rm p}-\eta_{\rm p}\varrho_0)^2}{2\varrho_0(\rho_{\rm p}-\varrho_0)}\right),\end{aligned} \tag{20}$$

  corresponding to the axial component of a projectile trajectory in the comoving frame where the center of mass moves along the z-axis with the speed $V_{\rm cm}$. The boosted projectile trajectory is now fully determined:

$$\mathbf{r}_{\rm p}(\rho_{\rm p}) = \rho_{\rm p}\hat{\boldsymbol{\rho}} + [\mathcal{Z}_{\rm p}(\rho_{\rm p}) + \mathcal{Z}_0]\hat{\mathbf{z}} \tag{21}$$

  as a function of a radial distance $\rho_{\rm p}$ from the z-axis.

4. Scattering shadow

We now ask: at the radial distance $\rho_{\rm p}$ from the $\mathcal{Z}$-axis, which trajectory reaches an extremal distance along the same axis (i.e. the extremal distance from the xy-plane), thus defining the point along the shadow caustic?

The problem boils down to finding the extremum[2] of $\mathcal{Z}_{\rm p}(\rho_{\rm p})$ in respect to the impact parameter ϱ_0, for a constant $\rho_{\rm p}$. This is done by finding the zero of the associated derivative, i.e. by

[2] The only (and inconsequential) difference in respect to the extremization procedure from [5] is that the angular parameter θ was kept constant therein, as in both the fixed-target and the center-of-mass frame it corresponds to a true angular coordinate. In any particular frame the extremization procedure must be performed by keeping some appropriate geometric parameter *from the same frame* constant, as we are interested in the point of the extremal approach (among all possible trajectories) to a given point, axis or plane *within that frame*. Since we already have an explicit dependence $\mathcal{Z}_{\rm p}(\rho_{\rm p})$ from (20), we can directly extremize the trajectories' distance from the xy-plane by keeping $\rho_{\rm p}$ constant, instead of first having to find the angular coordinate $\theta_{\rm p} = \operatorname{arccot}(\mathcal{Z}_{\rm p}/\rho_{\rm p})$ and then having to extremize the distance from the coordinate origin by keeping $\theta_{\rm p}$ constant. In that, it should be noted that the extremization procedure from [5] was a *minimization* of the distance from the coordinate origin, while (22) leads to the *maximization* of the trajectories' reach in the $\mathcal{Z}$-direction, and only because of the selected direction of the initial projectile velocity.

solving:

$$\left.\frac{\mathrm{d}\mathcal{Z}_\mathrm{p}}{\mathrm{d}\varrho_0}\right|_{\tilde{\varrho}_0} = \big\{(\eta_\mathrm{t} v_0 + V_\mathrm{cm})\tilde{\varrho}_0^2(\rho_\mathrm{p} - 2\tilde{\varrho}_0)(\rho_\mathrm{p} - \tilde{\varrho}_0)^2 + \big[\eta_\mathrm{t}(\eta_\mathrm{t} v_0 + V_\mathrm{cm})\tilde{\varrho}_0 - (\eta_\mathrm{t} v_0 - V_\mathrm{cm})(\rho_\mathrm{p} - \tilde{\varrho}_0)\big] \times \chi^2\rho_\mathrm{p}(\eta_\mathrm{p}\tilde{\varrho}_0 - \rho_\mathrm{p})\big\} \big/ \big[2\eta_\mathrm{t} v_0 \chi \tilde{\varrho}_0^2(\rho_\mathrm{p} - \tilde{\varrho}_0)^2\big] = 0 \tag{22}$$

for $\tilde{\varrho}_0$. We see that, in general case, we need to find the zero(s) of the 5th degree polynomial in $\tilde{\varrho}_0$. The general solution cannot be expressed in radicals. Even if it could, already the general solutions to the 3rd and 4th degree polynomial (Cardano formula and Ferrari method, respectively) are excessively long and incomprehensible. Therefore, we need to proceed numerically from this point.

In order to avoid the confusion between the trajectory equation $\mathcal{Z}_\mathrm{p}(\rho_\mathrm{p}; \varrho_0)$ and the shadow equation, we will use the notation $\mathbb{Z}_\mathrm{p}(\rho_\mathrm{p})$ for shadow caustic, in a sense:

$$\mathbb{Z}_\mathrm{p}(\rho_\mathrm{p}) \equiv \mathcal{Z}_\mathrm{p}[\rho_\mathrm{p}; \tilde{\varrho}_0(\rho_\mathrm{p})]. \tag{23}$$

Evidently, the shadow caustic is obtained by adopting the extremizing value $\tilde{\varrho}_0(\rho_\mathrm{p})$ from (22). There is one constraint upon the sought solution:

$$0 \leqslant \tilde{\varrho}_0(\rho_\mathrm{p}) \leqslant \rho_\mathrm{p}, \tag{24}$$

that one might hope to use in eliminating the spurious solutions. It follows from purely geometric considerations: in order to have reached the radial distance ρ_p, the projectile must have started from a lesser $\tilde{\varrho}_0$, due to the repulsive scattering away from the z-axis. However, there may still be multiple branches $\tilde{\varrho}_0^{(i)}$ consistent with (24), among which only one yields a sought solution at any given point. A detailed numerical investigation leads to a simple procedure for obtaining the shadow boundary under such conditions:

$$\mathbb{Z}_\mathrm{p}(\rho_\mathrm{p}) = \max_i \left\{\mathcal{Z}_\mathrm{p}[\rho_\mathrm{p}; \tilde{\varrho}_0^{(i)}(\rho_\mathrm{p})]\right\}, \tag{25}$$

where i enumerates all the solutions consistent with (24). The basic reasoning behind this procedure may be easily understood. All nonnegative solutions to the extremization problem (22) do indeed yield some meaningful, local extremum. However, the shadow caustic is determined by the global maximum, beyond which no additional trajectories are to be found (we recall that the maximum is the relevant extremum only because of the selected direction of initial projectile velocity). Thus, beyond the maximum of all local extrema no other extremum, as a candidate for a point on a shadow caustic, can be found.

5. Existence conditions

Let us try to anticipate any possible conditions for the existence of the scattering shadow in a given comoving frame. In attempting this, a shadow vertex—a single shadow point lying on the $\mathcal{Z}$-axis, i.e. $\mathbb{Z}_\mathrm{p}(\rho_\mathrm{p} = 0)$—will be of special importance. To this end let us consider what happens with the projectile trajectory impinging frontally upon the target ($\varrho_0 = 0$). It is to be noted that the shadow vertex is completely determined by precisely this one trajectory, which is entirely confined along the $\mathcal{Z}$-axis. If, in a given comoving frame, the projectile with the impact parameter $\varrho_0 = 0$ can be backscattered (recoiled backwards off the target), then the shadow vertex stays at some finite position along the $\mathcal{Z}$-axis. On the other hand, if the backscattering

is kinematically impossible (due to the projectile being too massive or the forward center-of-mass speed $V_{\rm cm}$ being too high), the projectile keeps moving in a forward direction, implying that the shadow vertex escapes to infinity, even after the primary shift to infinity by $\mathcal{Z}_0$!

It is now a simple matter to argue that if the $\varrho_0 = 0$ trajectory is entirely forward directed, than all other $\varrho_0 > 0$ trajectories also retain the forward motion without ever bending backwards. To this end we first consider the motion in the center-of-mass frame. At the initial moment all projectiles are put into motion with the velocity $\mathbf{v}_{\rm p}^{\rm (cm)}(0) = \eta_{\rm t} v_0 \hat{\mathbf{z}}$. This speed value also corresponds to a maximum speed component $\mathcal{V}_z^{\rm (max)}$ along the same axis, for any trajectory and among all trajectories (for any ϱ_0):

$$\mathcal{V}_z^{\rm (max)} \equiv \max_{t,\varrho_0} \left[\mathbf{v}_{\rm p}^{\rm (cm)}(t;\varrho_0)\right]_z = \left[\mathbf{v}_{\rm p}^{\rm (cm)}(0;\varrho_0)\right]_z = \eta_{\rm t} v_0. \tag{26}$$

The same speed is also reached asymptotically by all projectile trajectories: $v_{\rm p}^{\rm (cm)}(\infty) = \eta_{\rm t} v_0$. Yet, due to the particular scattering angle, only for the frontal trajectory ($\varrho_0 = 0$) is the final velocity directed entirely along the z-axis, meaning that this particular case yields the minimum speed component $\mathcal{V}_z^{\rm (min)}$, for this particular trajectory and among all possible trajectories:

$$\mathcal{V}_z^{\rm (min)} \equiv \min_{t,\varrho_0} \left[\mathbf{v}_{\rm p}^{\rm (cm)}(t;\varrho_0)\right]_z = \left[\mathbf{v}_{\rm p}^{\rm (cm)}(\infty;0)\right]_z = -\eta_{\rm t} v_0. \tag{27}$$

Therefore, if the center-of-mass speed $V_{\rm cm}$ is sufficient to boost forward the asymptotic state of the frontal trajectory (i.e. if $\mathcal{V}_z^{\rm (min)} + V_{\rm cm} \geqslant 0$, being equivalent to $V_{\rm cm} \geqslant \eta_{\rm t} v_0$) then all other trajectories will also be forward directed. This has a remarkable consequence: there will be no back-bending of any trajectory, so that when the frontal trajectory escapes to infinity (beyond $\mathcal{Z}_0$), there is a continuum of entirely-forward-directed trajectories sweeping the entire geometric space. Thus, the scattering shadow cannot exist at all in comoving frames with $V_{\rm cm} \geqslant \eta_{\rm t} v_0$!

There is another extreme to this condition. As $\mathcal{V}_z^{\rm (max)}$ is the maximum speed along the z-axis for any and all trajectories, consider what happens when $\mathcal{V}_z^{\rm (max)} + V_{\rm cm} \leqslant 0$, i.e. when $V_{\rm cm} \leqslant -\eta_{\rm t} v_0$. In such frames all the projectiles are immediately boosted backwards and the entire geometric space beyond their initial position is shielded from their trajectories. This means that the scattering shadow spans the entire geometric space. Its form may still be properly parameterized, being trivial in itself. One only needs to note that the shadow caustic is now a plane spanning the geometric place of all initial projectile positions. Ever since (16), we have had these positions parameterized as: $z_{\rm p}(t = 0;\varrho_0) = -\lim_{z_0\to\infty} z_0$. By the virtue of (19) and (23) we may immediately write:

$$\mathbb{Z}_{\rm p}(\rho_{\rm p}; V_{\rm cm} \leqslant -\eta_{\rm t} v_0) = -\lim_{z_0\to\infty} z_0 - \mathcal{Z}_0, \tag{28}$$

which we call a *trivial* scattering shadow[3].

[3] It is not as trivial to obtain it formally as a limit $\lim_{V_{\rm cm}\to-\eta_{\rm t}v_0} \mathbb{Z}_{\rm p}(\rho_{\rm p}; V_{\rm cm})$ of the procedure from the section 4. Taking another glance at (22), we may notice that precisely in the limiting case $V_{\rm cm} = -\eta_{\rm t} v_0$ the extremization condition simplifies from the 5th degree to the 2nd degree polynomial, i.e. the quadratic equation in $\tilde{\varrho}_0$, yielding the two solutions: $\tilde{\varrho}_0^{(1)} = \rho_{\rm p}$ and $\tilde{\varrho}_0^{(2)} = \rho_{\rm p}/\eta_{\rm p}$. The second solution is clearly unacceptable, as seen from (24), since $0 \leqslant \eta_{\rm p} \leqslant 1$. Though the first solution is also unacceptable—as $\tilde{\varrho}_0 = \rho_{\rm p}$ can only be for the frontal trajectory ($\varrho_0 = 0$)—it clearly represents the limit of the acceptable solutions, as $V_{\rm cm}$ approaches $-\eta_{\rm t} v_0$. However, one can easily check that plugging this solution into (23) does not help in identifying the trivial-shadow equation (28), due to no apparent connection between $\rho_{\rm p} - \tilde{\varrho}_0$ and z_0 in the limit $V_{\rm cm} \to -\eta_{\rm t} v_0$. Finally, it is interesting to explicitly state the physical meaning behind the frame defined by $V_{\rm cm} = -\eta_{\rm t} v_0$. From the definition of the center-of-mass speed we can easily see that in this frame, instead of the target, the projectile is at rest at the initial moment. Thus, we may think of it as the inverse-laboratory frame.

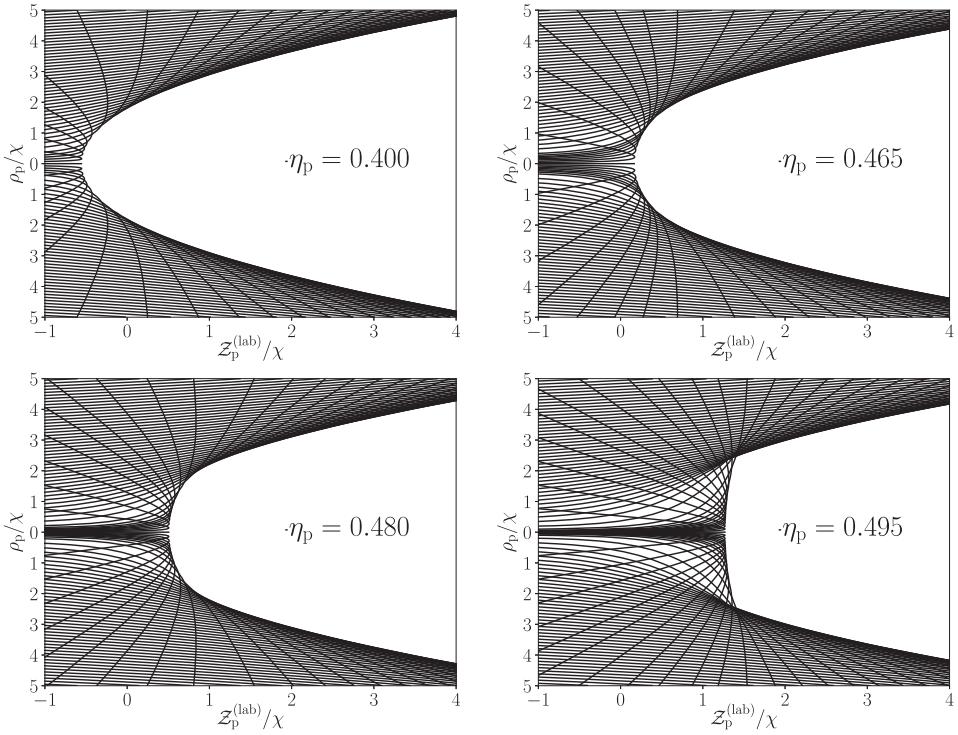

Figure 1. Examples of the projectile trajectories in the laboratory frame for several selected values of η_p. The trajectories' envelope forms a scattering shadow caustic. For visual purposes the impact parameters are not all selected as equidistant, thus the plots do not display the true density of the trajectories. For each separate value of η_p, the origin shift $\mathcal{Z}_0$ from (18) is different, therefore the care should be taken in interpreting the transformed coordinate $\mathcal{Z}_\mathrm{p}^{(\mathrm{lab})}$. The scattering shadow in the laboratory frame exists only for $\eta_\mathrm{p} < 0.5$, otherwise the trajectories sweep the entire geometric space.

In summary, the scattering shadow in the comoving frame can exist and take a nontrivial form if and only if:

$$-\eta_\mathrm{t} v_0 < V_\mathrm{cm} < \eta_\mathrm{t} v_0 \quad \Leftrightarrow \quad \eta_\mathrm{t} > \frac{|V_\mathrm{cm}|}{v_0}. \tag{29}$$

The left expression is to be interpreted as the condition upon the center-of-mass speed, given the projectile and target masses. The right expression is the condition upon their respective masses, given the center-of-mass speed. Since $0 \leqslant \eta_\mathrm{t} \leqslant 1$, these conditions mean that there cannot possibly exist a (nontrivial) scattering shadow in the comoving frames such that $|V_\mathrm{cm}| \geqslant v_0$, regardless of the selection of the projectile and target masses.

6. Laboratory frame

In this section we commit ourselves to the laboratory frame, where the target is at rest at the initial moment: $v_\mathrm{t}^{(\mathrm{lab})}(0) = 0$. Since the projectile carries all of the initial relative speed: $v_\mathrm{p}^{(\mathrm{lab})}(0) = v_0$, the center-of-mass speed in the laboratory frame is: $V_\mathrm{cm}^{(\mathrm{lab})} = \eta_\mathrm{p} v_0$. Plugging this into (20) and choosing $\mathcal{L} = \chi$ for an arbitrary length scale, we obtain the particle trajectories

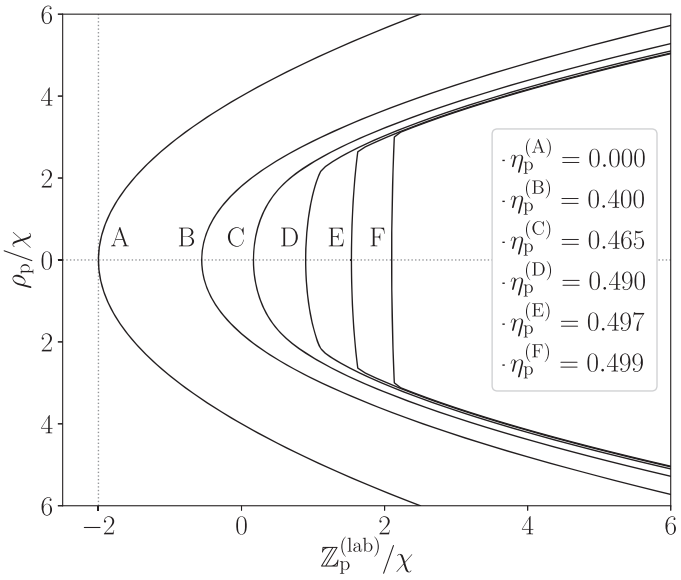

Figure 2. Examples of the scattering shadow in the laboratory frame, obtained by solving (32) for $\tilde{\varrho}_0$ and employing (25). The shadow exists in the laboratory frame only for $\eta_\mathrm{p} < 0.5$. The relative positioning of shadows in a transformed coordinate $\mathbb{Z}_\mathrm{p}^{(\mathrm{lab})}$ does not reflect their true geometric positioning. The case $\eta_\mathrm{p}^{(\mathrm{A})} = 0$ corresponds to an infinitely massive target, when the laboratory frame coincides both with the fixed-target and the center-of-mass frame, with the shadow taking a simple paraboloidal form $\mathbb{Z}_\mathrm{p}^{(\mathrm{lab})}/\chi = (\rho_\mathrm{p}/\chi)^2/8 - 2$ from [5].

in the laboratory frame:

$$\mathcal{Z}_\mathrm{p}^{(\mathrm{lab})}(\rho_\mathrm{p}) = \frac{\chi(\rho_\mathrm{p} - \eta_\mathrm{p}\varrho_0)[(\eta_\mathrm{p} - \eta_\mathrm{t})\rho_\mathrm{p} - \eta_\mathrm{p}\varrho_0]}{2\eta_\mathrm{t}\varrho_0(\rho_\mathrm{p} - \varrho_0)} + \frac{\varrho_0(\rho_\mathrm{p} - \varrho_0)}{2\eta_\mathrm{t}\chi} + \eta_\mathrm{p}\chi \ln\frac{\rho_\mathrm{p} - \varrho_0}{\eta_\mathrm{t}\varrho_0}. \quad (30)$$

It should be noted that after selecting the natural scale $\mathcal{L} = \chi$, the trajectory and all the results following from it may be expressed in a scaled, dimensionless coordinates $\bar{x} \equiv x/\chi$, where $x \in \{\varrho_0, \rho_{\mathrm{p,t}}, z_{\mathrm{p,t}}, \mathcal{Z}_{\mathrm{p,t}}, \mathbb{Z}_{\mathrm{p,t}}, \dots\}$. Though this universal form—independent of the underlying parameters from χ—may already be applied to a general case from (20), for illustrative purposes we only give the example of a scaled version of (30):

$$\bar{\mathcal{Z}}_\mathrm{p}^{(\mathrm{lab})}(\bar{\rho}_\mathrm{p}) = \frac{(\bar{\rho}_\mathrm{p} - \eta_\mathrm{p}\bar{\varrho}_0)[(\eta_\mathrm{p} - \eta_\mathrm{t})\bar{\rho}_\mathrm{p} - \eta_\mathrm{p}\bar{\varrho}_0]}{2\eta_\mathrm{t}\bar{\varrho}_0(\bar{\rho}_\mathrm{p} - \bar{\varrho}_0)} + \frac{\bar{\varrho}_0(\bar{\rho}_\mathrm{p} - \bar{\varrho}_0)}{2\eta_\mathrm{t}} + \eta_\mathrm{p} \ln\frac{\bar{\rho}_\mathrm{p} - \bar{\varrho}_0}{\eta_\mathrm{t}\bar{\varrho}_0}. \quad (31)$$

We use such scaled coordinates for displaying all graphical results. In that, figure 1 shows examples of the projectile trajectories in the laboratory frame—according to (31)—for several values of η_p. According to the existence conditions from (29) the scattering shadow in the laboratory frame exists only for $\eta_\mathrm{p} < 0.5$.

Figure 2 recovers several selected shadow forms directly, by following all the steps required by the shadow determination procedure from (25). The central part of this procedure is the numerical identification of the relevant roots to the 5th degree polynomial from the associated

extremization condition for determining $\tilde{\varrho}_0$:

$$\left.\frac{\mathrm{d}\mathcal{Z}_\mathrm{p}^{(\mathrm{lab})}}{\mathrm{d}\varrho_0}\right|_{\tilde{\varrho}_0} = \left\{\tilde{\varrho}_0^2(\rho_\mathrm{p}-2\tilde{\varrho}_0)(\rho_\mathrm{p}-\tilde{\varrho}_0)^2-\chi^2\rho_\mathrm{p}\left[\eta_\mathrm{p}(\eta_\mathrm{p}-2\eta_\mathrm{t})\varrho_0^2+2(\eta_\mathrm{t}-\eta_\mathrm{p}^2)\varrho_0\rho_\mathrm{p}\right.\right.$$
$$\left.\left.+(\eta_\mathrm{p}-\eta_\mathrm{t})\rho_\mathrm{p}^2\right]\right\}\Big/\left[2\eta_\mathrm{t}\chi\tilde{\varrho}_0^2(\rho_\mathrm{p}-\tilde{\varrho}_0)^2\right]=0. \tag{32}$$

It should be noted that both in figures 1 and 2 each particular shadow has been shifted by a separate value of $\mathcal{Z}_0$, so that in a transformed coordinate $\mathcal{Z}_\mathrm{p}$ the separate shadows do not reflect their true relative geometric positioning, as they do in a true spatial coordinate z_p.

Something remarkable may be observed in figures 1 and 2. For the values of η_p above approximately 0.49 there is a discontinuity among the projectile trajectories which contribute to the formation of a shadow caustic, causing the scattering shadow to exhibit a sharp edge. This is indeed the case and not just the visual artifact. The sudden breakdown of the shadow smoothness is directly related to a qualitative change in the behavior of solutions to the extremization problem (22) and the appearance of the multiple roots $\tilde{\varrho}_0^{(i)}$ consistent with (24). Singling out the relevant root is the precise purpose of the method from (25). Based on these observations, one can rightly claim that this effect has a mathematical form of a phase transition—a new and by no means obvious phenomenon that does not manifest itself either in the fixed-target or the center-of-mass frame.

For a few selected values of η_p, figure 3 shows the behavior of the solutions $\tilde{\varrho}_0(\rho_\mathrm{p})$—consistent with (24)—to the extremization condition (32) from the laboratory frame. In order to reinforce the notion of a phase transition, at least by mathematical analogy, the inverse dependence $\rho_\mathrm{p}(\tilde{\varrho}_0)$ is deliberately shown, so as to remind the reader of a phase transition in a well known van der Waals equation of state, describing the thermodynamic behavior of real gases. Within this analogy, each curve from figure 3 is reminiscent of a particular isotherm from a pressure-volume diagram of the van der Waals model. Thus, the following analogies may be identified between its thermodynamic parameters—temperature T, (molar) volume V and pressure p—and the Rutherford scattering parameters: $\eta_{\mathrm{p/t}} \leftrightarrow T$, $\tilde{\varrho}_0 \leftrightarrow V$ and $\rho_\mathrm{p} \leftrightarrow p$.

A phase transition in the van der Waals model clearly corresponds to a thermodynamic transition between the liquid and gaseous state of matter. A physical interpretation of a phase transition in the Rutherford scattering shadow is more difficult to identify. The reason is the nature of parameters governing the phase states. The phase transition in the scattering shadow can be achieved (1) by varying the projectile/target mass ratio from η_p, (2) by varying the ratio V_cm/v_0 of relevant speeds[4], thus switching between the comoving frames, (3) or by varying both ratios simultaneously, as in the case of all possible laboratory frames, defined by $V_\mathrm{cm}^{(\mathrm{lab})}/v_0 = \eta_\mathrm{p}$. Unlike the thermodynamic parameters from the van der Waals model, the projectile and target masses can hardly be varied—either continuously or at all—thus obscuring the physical interpretation of the phase transition by precluding its realization in practice. On the other hand, inducing a phase transition by switching between the comoving frames makes both the shadow itself and (the possibility of) its phase transition observer-dependent. This means that the shadow phase is determined by the observer's point of view, rather than being

[4] It is shown in section F of the supplementary note that for a given mass ratio (η_p or, equivalently, η_t) one can always achieve a phase transition by varying the ratio V_cm/v_0. However, for a given V_cm/v_0 one can achieve a phase transition by varying the mass ratio only if $V_\mathrm{cm}/\eta_\mathrm{t}v_0 \notin [0, 6\sqrt{15}/25] \approx [0, 0.9295]$. This demonstration is outside of the scope of calculations presented herein.

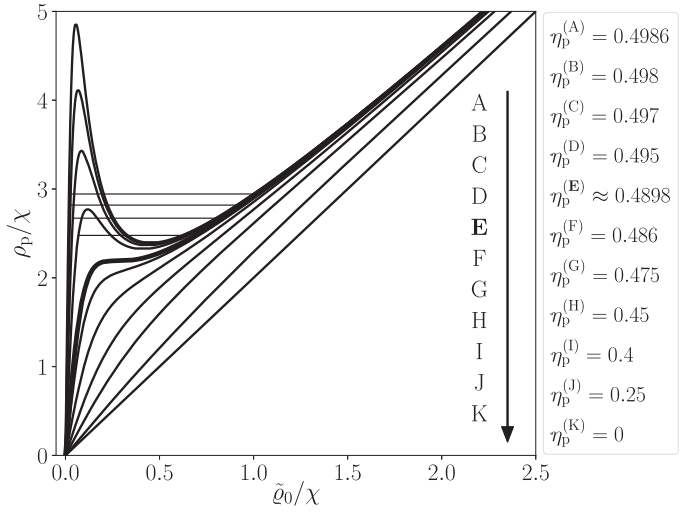

Figure 3. Solutions $\tilde{\varrho}_0(\rho_p)$—consistent with (24)—to the extremization condition (32) from the laboratory frame, for different values of the projectile/target mass ratio, expressed through η_p. Inverse dependence $\rho_p(\tilde{\varrho}_0)$ is shown in order to illustrate the analogy with the thermodynamic van der Waals model. Cases A–D show a split shadow phase; cases F–K show a smooth shadow phase. Case **E** (a thick line) corresponds to a critical value of η_p, when a phase transition between the shadow phase states occurs. Examples of the Maxwellian construction are shown by horizontal line segments.

an intrinsic property of the scattering shadow itself, again obstructing the physical interpretation of its phase transition. For this reason it should be reemphasized that the phase transition in the scattering shadow is only a matter of a mathematical analogy, lacking in physically meaningful 'parameters of state' that would uniquely determine the shadow state upon which all observers could agree. Rather, the phase transition occurs in the observer's own kinematic relation to (and in his/her own perception of) the portion of space shielded from the projectile trajectories. This is because—for simultaneously released projectiles—the shadow caustic is not formed simultaneously. It ensues from the intersection of the trajectories' geometric forms, without them actually passing through the same point in space at the same point in time. For a moving observer different points alongside the projectile trajectory are shifted by a different amount ($\mathbf{V}_{cm}t$), thus affecting the shape of the entire trajectory, rather than just translating it between the frames in relative motion. Since the trajectories themselves deform, so does the locus of their geometric intersections. This justifies any and all shadow caustic distortions between the frames in relative motion, including the possibility of a sudden and significant qualitative change, mathematically manifested as a type of a phase transition.

We have already noted that after selecting the natural scale $\mathcal{L} = \chi$ in (18) and (20), just as we have done in (30), the Rutherford scattering problem becomes scale invariant. Van der Waals equation also exhibits the scale invariance when expressed in terms of the so-called reduced thermodynamic variables: $(\bar{p} + 3/\bar{V}^2)(3\bar{V} - 1) = 8\bar{T}$, each scaled by an appropriate critical value: $\bar{T} = T/T_c$, $\bar{p}/p_c$, $\bar{V} = V/V_c$. By now it should not be surprising at all that that the phase transition in the scattering shadow also features its own (analogies of) critical parameters. Axes labels in figure 3 help in observing that for both ρ_p and $\tilde{\varrho}_0$ the analogy of the critical, scaling parameter is the length scale χ. The existence and the value of the critical projectile/target mass ratio is dependent on a particular comoving frame, but when it exists it is a critical value in

a true sense. The constraint $V_{\mathrm{cm}}^{(\mathrm{lab})} = \eta_{\mathrm{p}} v_0$ defining the laboratory frame for a particular value of η_{p} is such that the critical value of η_{p} does exist among all possible laboratory frames (for different η_{p}). In figure 3 the critical value $\eta_{\mathrm{p}} \approx 0.489\,756$, i.e. $m_{\mathrm{p}}/m_{\mathrm{t}} \approx 0.959\,846$ is illustrated by a thick line corresponding to the case **E**.

The parallels with the van der Waals model go so far that the phase transition in the scattering shadow even features its own analogy of the Maxwell construction. Within the van der Waals model the Maxwell construction consists of a manual correction of the smooth but unphysical $p(V)$ dependence below the critical temperature T_{c}, when the phase transition just becomes possible to achieve. The analogy of the Maxwell construction for the scattering shadow—that we call a Maxwellian construction—comes about as a consequence of the recipe (25) for selecting the appropriate, shadow related solution $\tilde{\varrho}_0$. In figure 3 the examples of the Maxwellian construction are shown by horizontal segments, appearing beyond (and only beyond) the critical value of η_{p}. In case of the scattering shadow the solution $\tilde{\varrho}_0(\rho_{\mathrm{p}})$ discontinuously switches between the leftmost and rightmost branch, so that no solution $\tilde{\varrho}_0$, i.e. no projectile trajectory within the range of Maxwellian construction takes part the shadow formation. Precisely this discontinuity leads to the appearance of a sharp edge along the shadow caustic.

There are two related differences in respect to the van der Waals model that need to be clarified, so as to avoid any confusion. The first, inessential one is a matter of nomenclature: what we regard as a phase transition, i.e. what we consider as distinct phases in the scattering shadow. The second, essential one is related to the attainability of the thermodynamic states along the Maxwell construction and of the solutions $\tilde{\varrho}_0(\rho_{\mathrm{p}})$ along the Maxwellian construction. In the van der Waals model the $p(V)$ dependences from each side of the Maxwell construction correspond to the separate, liquid and gaseous phase states. The Maxwell construction corresponds to a phase transition itself, representing a realistic mixture of these phase states, through which the evolution of a thermodynamic system progresses in reality. In case of the scattering shadow we consider the entire $\tilde{\varrho}_0(\rho_{\mathrm{p}})$ dependences for particular values of η_{p} as separate phases, based on the (non)existence of the sharp edge along the shadow caustic. Recalling the shadow existence condition (29), we distinguish between four phase states: a smooth shadow phase, a split shadow phase, a trivial shadow phase and no shadow phase. In this sense, only the critical line (case **E**) from figure 3 represents the phase transition, between a split (cases A–D) and a smooth (cases F–K) shadow. It also bears repeating that the solutions $\tilde{\varrho}_0(\rho_{\mathrm{p}})$ along the Maxwellian construction are excluded from the shadow formation, i.e. are not attainable in a sense of a liquid–gas mixture from the van der Waals model. In a direct analogy with the van der Walls model, the smooth shadow would represent a pure gaseous state, the only one present above the critical temperature. Within the split shadow phase the sharp edge along the shadow caustic—manifested in the Maxwellian construction—would correspond to the mixture of phase states, while the two split shadow branches would correspond to a pure liquid and a pure gaseous state. In that, the branch containing the shadow vertex ($\rho_{\mathrm{p}} = 0$) is reminiscent of a liquid state—as its portion increases by driving the relevant η_{p} parameter away from the smooth shadow phase—leaving the other, asymptotically paraboloidal branch to represent a gaseous state. If one's imagination was let to run free, one could make further comparisons of a trivial and no shadow phase with the plasma and solid state of matter, respectively.

7. Conclusion

We have established a method for obtaining the Rutherford scattering shadow in the comoving frame—an inertial frame moving along the initial projectile direction, with the charged target initially being at the origin of the frame. The laboratory frame fits this categorization perfectly,

being defined by an additional requirement that the target be initially at rest. The method itself consists of the extermization procedure related to the projectile trajectories in the comoving frame and involves solving the 5th degree polynomial. We have identified the condition for the existence of the (nontrivial) scattering shadow in a given comoving frame, which puts a limitation on its speed of motion, relative to the center-of-mass frame. The trivial scattering shadow refers to the entire geometric space being shadowed, when all the projectile trajectories are immediately boosted backwards due to the excessive center-of-mass speed in a backward direction. In the laboratory frame, in particular, the scattering shadow exists only if the target is more massive than the projectile ($m_\mathrm{t} > m_\mathrm{p}$). Otherwise, the projectile trajectories sweep the entire geometric space, not forming any shadow at all. A new phenomenon was identified, related to a transition between the comoving frames or, alternatively, to a varying ratio of the projectile and target masses. It consists of a phase transition between an entirely smooth type of scattering shadow and the one characterized by a loss of smoothness at the point where the shadow caustic splits, forming a sharp edge. This finding shows that the transition between the frames is not just a technical challenge to be carried out for the sake of completeness. Rather, it is a rewarding venture, offering a novel insight into otherwise well known scattering process.

Appendix A. Derivation of the Coulomb trajectories in the comoving frame

We need to determine the time dependence of the trajectories in order to be able to boost them via the $\mathbf{R}(t)$ term from (15). We start from (see, for example [5]):

$$\frac{\mathrm{d}\theta}{\mathrm{d}t} = -\frac{\varrho_0 v_0}{r^2(\theta)} \quad \Rightarrow \quad \int_0^{t(\theta)} \mathrm{d}t' = -\frac{1}{\varrho_0 v_0} \lim_{\theta_0 \to \pi} \int_{\theta_0}^{\theta} r^2(\theta') \mathrm{d}\theta', \tag{A.1}$$

which is equivalent to the conservation of the angular momentum. It is to be noted that the angular coordinate θ is still the one from the fixed-target frame and will remain so throughout the entirety of our calculations. Therefore, it is not to be confused with the actual angular coordinate from the given comoving frame. Since the initial angular coordinate of the projectile ($\theta_0 \to \pi$) leads to the divergence in the right-hand-side integral, based on (16) we parameterize it as: $\lim_{\theta_0 \to \pi} \theta_0 = \pi - \lim_{z_0 \to \infty} \arctan(\varrho_0 / z_0)$, so that:

$$t(\theta) = -\frac{1}{\varrho_0 v_0} \lim_{z_0 \to \infty} \int_{\pi - \arctan(\varrho_0/z_0)}^{\theta} r^2(\theta') \mathrm{d}\theta'. \tag{A.2}$$

It should be stated that for finite z_0 (i.e. $\theta_0 \not\to \pi$) the solution (10) for $r(\theta)$ does not hold any more. However, we will keep z_0 infinite at all times, while this parameterization only serves to do so in a strictly controlled and formally correct manner. The antiderivative of $r^2(\theta)$ is:

$$\int^{\theta} r^2(\theta') \mathrm{d}\theta' = -\left(\varrho_0 \cos\theta + \chi \sin\theta\right) r(\theta) + \chi \varrho_0 \ln\left[\left(\varrho_0 \tan\frac{\theta}{2} - \chi\right)/\mathcal{L}\right], \tag{A.3}$$

with $\mathcal{L}$ as an arbitrary length scale, formally required for an argument of the logarithm to be dimensionless. In entering the lower integration bound from (A.2) we make use of the following limits:

$$\lim_{\theta_0 \to \pi} r(\theta_0) \sin\theta_0 = \varrho_0, \tag{A.4}$$

$$\lim_{\theta_0 \to \pi} r(\theta_0) \cos\theta_0 = -\lim_{z_0 \to \infty} z_0, \tag{A.5}$$

$$\lim_{\theta_0\to\pi} \ln \frac{\varrho_0 \tan\frac{\theta_0}{2} - \chi}{\mathcal{L}} = \lim_{z_0\to\infty} \ln \frac{2z_0}{\mathcal{L}}. \tag{A.6}$$

Using these in the context of (A.2), we have:

$$t(\theta) = \frac{1}{v_0}\left[\left(\cos\theta + \frac{\chi}{\varrho_0}\sin\theta\right) r(\theta) - \chi \ln\left[\left(\varrho_0 \tan\frac{\theta}{2} - \chi\right)/\mathcal{L}\right] + \lim_{z_0\to\infty} z_0 + \chi \lim_{z_0\to\infty} \ln\left(2z_0/\mathrm{e}\mathcal{L}\right)\right]. \tag{A.7}$$

Here we have absorbed an additional $-\chi$ term—related to the limit (A.4)—within the last logarithm by introducing the natural logarithm base e (not to be confused with the unit charge e).

Combining (13) and (16), and recalling that $\mathbf{R}_0 = \eta_\mathrm{p}\mathbf{r}_\mathrm{p}(t=0)$, a particle trajectory in an arbitrary comoving frame where the center of mass moves along the z-axis with the velocity $\mathbf{V}_\mathrm{cm} = V_\mathrm{cm}\hat{\mathbf{z}}$:

$$\mathbf{r}_\mathrm{p}(\theta) = \mathbf{R}_0 + \mathbf{V}_\mathrm{cm} t(\theta) + \eta_\mathrm{t}\mathbf{r}(\theta) \tag{A.8}$$

is easily decomposed into the cylindrical components as:

$$\rho_\mathrm{p}(\theta) = \mathbf{r}_\mathrm{p}(\theta)\cdot\hat{\boldsymbol{\rho}} = \eta_\mathrm{p}\varrho_0 + \eta_\mathrm{t} r(\theta)\sin\theta, \tag{A.9}$$

together with:

$$z_\mathrm{p}(\theta) = \mathbf{r}_\mathrm{p}(\theta)\cdot\hat{\mathbf{z}} = -\eta_\mathrm{p}\lim_{z_0\to\infty} z_0 + V_\mathrm{cm} t(\theta) + \eta_\mathrm{t} r(\theta)\cos\theta = \mathcal{Z}_\mathrm{p}(\theta) + \mathcal{Z}_0, \tag{A.10}$$

where we have absorbed all the infinities into:

$$\mathcal{Z}_0 \equiv \left(\frac{V_\mathrm{cm}}{v_0} - \eta_\mathrm{p}\right)\lim_{z_0\to\infty} z_0 + \frac{V_\mathrm{cm}}{v_0}\chi \lim_{z_0\to\infty} \ln\frac{2z_0}{\mathrm{e}\mathcal{L}}, \tag{A.11}$$

and isolated all the relevant dependence by:

$$\mathcal{Z}_\mathrm{p}(\theta) \equiv \left(\frac{V_\mathrm{cm}}{v_0} + \eta_\mathrm{t}\right) r(\theta)\cos\theta + \frac{V_\mathrm{cm}}{v_0}\frac{\chi}{\varrho_0} r(\theta)\sin\theta - \frac{V_\mathrm{cm}}{v_0}\chi \ln\left[\left(\varrho_0 \tan\frac{\theta}{2} - \chi\right)/\mathcal{L}\right]. \tag{A.12}$$

It bears repeating that the angle θ is still the one from the fixed-target frame, parameterizing the trajectory in a selected comoving frame. This is precisely why the projections of a target-relative projectile position $\mathbf{r}(\theta)$ may be and have been performed simply by taking $r(\theta)\sin\theta$ and $r(\theta)\cos\theta$. From $\mathcal{Z}_0$ and $\mathbf{r}_\mathrm{t} = \mathbf{r}_\mathrm{p} - \mathbf{r}$ we see that that the Coulomb interaction is strong enough that the target is pushed infinitely far by a recoil before the projectile manages to approach it at some finite distance ($\theta < \pi$). This may have been suspected, but not *a priori* expected from the fixed-target and the center-of-mass frame. In all frames the infinite distance must be negotiated between the projectile and the target, but that does not mean in advance that the target itself is shifted by an infinite distance from its initial position. Seeing now that it is in any of the comoving frames, we introduced the new coordinate origin $\mathcal{Z}_0$, thus defining the new, transformed coordinate $\mathcal{Z} \equiv z - \mathcal{Z}_0$. In other words, we are now observing the scattering around the point $\mathcal{Z}_0$ at an infinite distance from the target's initial position, so that the transformed coordinate $\mathcal{Z}$ is entirely under control. Since θ is an angular coordinate from the fixed-target

frame, rather than from the comoving frame, no geometric redefinition of it needs to take place due to this origin shift.

We now have the projectile trajectory parameterized by the cylindrical coordinates from (A.9) and (A.12), dependent on the angle θ from the fixed-target frame. In order to determine the scattering shadow in the comoving fame, we need to find the extremum of some specific trajectory distance by keeping fixed some geometric parameter from the same frame. For example, we might extremize the distance from the origin by keeping fixed an angle relative to the $\mathcal{Z}$-axis, or the distance along the $\mathcal{Z}$-axis by keeping fixed the distance ρ_p from the same axis. To this end, we aim to translate the dependence $\mathcal{Z}_\mathrm{p}(\theta)$ from (A.12) into $\mathcal{Z}_\mathrm{p}(\rho_\mathrm{p})$. For brevity of expressions we temporarily define the projectile distance from the z-axis in a fixed-target frame as:

$$\xi_\mathrm{p} \equiv \rho_\mathrm{p}^{(\mathrm{fix})} = r(\theta)\sin\,\theta. \tag{A.13}$$

Using (10), one easily obtains:

$$\xi_\mathrm{p} = \frac{\varrho_0^2\,\tan\,\frac{\theta}{2}}{\varrho_0\,\tan\,\frac{\theta}{2} - \chi} \quad \Rightarrow \quad \tan\,\frac{\theta}{2} = \frac{\chi\xi_\mathrm{p}}{\varrho_0(\xi_\mathrm{p} - \varrho_0)}, \tag{A.14}$$

so that:

$$r(\theta)\cos\,\theta = \frac{\varrho_0^2\left(1 - \tan^2\,\frac{\theta}{2}\right)}{2\left(\varrho_0\,\tan\,\frac{\theta}{2} - \chi\right)} = \frac{\varrho_0^2(\xi_\mathrm{p} - \varrho_0)^2 - \chi^2\xi_\mathrm{p}^2}{2\chi\varrho_0(\xi_\mathrm{p} - \varrho_0)}. \tag{A.15}$$

Combining these results within (A.12) and using the relation for $\xi_\mathrm{p}(\rho_\mathrm{p})$ from (A.9):

$$\xi_\mathrm{p}(\rho_\mathrm{p}) = \frac{\rho_\mathrm{p} - \eta_\mathrm{p}\varrho_0}{\eta_\mathrm{t}}, \tag{A.16}$$

we finally arrive at:

$$\begin{aligned}\mathcal{Z}_\mathrm{p}(\rho_\mathrm{p}) = {} & \frac{V_\mathrm{cm}}{v_0}\chi\left(\frac{\rho_\mathrm{p}}{\eta_\mathrm{t}\varrho_0} + \ln\,\frac{\mathcal{L}(\rho_\mathrm{p} - \varrho_0)}{\eta_\mathrm{t}\chi\varrho_0} - \frac{\eta_\mathrm{p}}{\eta_\mathrm{t}}\right) \\ & + \left(\frac{V_\mathrm{cm}}{\eta_\mathrm{t}v_0} + 1\right)\left(\frac{\varrho_0(\rho_\mathrm{p} - \varrho_0)}{2\chi} - \frac{\chi(\rho_\mathrm{p} - \eta_\mathrm{p}\varrho_0)^2}{2\varrho_0(\rho_\mathrm{p} - \varrho_0)}\right),\end{aligned} \tag{A.17}$$

which is a projectile trajectory in the comoving frame where the center of mass moves along the $\mathcal{Z}$-axis with the speed V_cm.

ORCID iDs

Petar Žugec https://orcid.org/0000-0001-6933-3100

References

[1] Geiger H 1908 On the scattering of the α-particles by matter *Proc. R. Soc.* A **81** 174–7
[2] Geiger H and Marsden E 1909 On a diffuse reflection of the α-particles *Proc. R. Soc.* A **82** 495–500
[3] Geiger H 1910 The scattering of α-particles by matter *Proc. R. Soc.* A **83** 492–504
[4] Rutherford E 1911 LXXIX. The scattering of α and β particles by matter and the structure of the atom *London, Edinburgh Dublin Phil. Mag. J. Sci.* **21** 669–88

[5] Žugec P and Topić I 2020 A shadow of the repulsive Rutherford scattering in the fixed-target and the center-of-mass frame *Eur. J. Phys.* **41** 065005
[6] Aono M and Souda R 1985 Quantitative surface atomic structure analysis by low-energy ion scattering spectroscopy (ISS) *Japan. J. Appl. Phys.* **24** 1249–62
[7] Brongersma H, Draxler M, Deridder M and Bauer P 2007 Surface composition analysis by low-energy ion scattering *Surf. Sci. Rep.* **62** 63–109
[8] Shatilov D A and Silagadze Z K 2021 A shadow of the repulsive Rutherford scattering and Hamilton vector *Eur. J. Phys.* **42** 035001
[9] Gu J and Chen C-C 2021 A geometric approach to the envelope of Coulomb orbits starting from a point in space *Eur. J. Phys.* **42** 055007
[10] Adolph J W, Garcia A L, Harter W G, McLaughlin G C, Shiffman R R and Surkus V G 1972 Some geometrical aspects of classical Coulomb scattering *Am. J. Phys.* **40** 1852–7
[11] Warner R E and Huttar L A 1991 The parabolic shadow of a Coulomb scatterer *Am. J. Phys.* **59** 755–6
[12] Samengo I and Barrachina R O 1994 Rainbow and glory scattering in Coulomb trajectories starting from a point in space *Eur. J. Phys.* **15** 300–8
[13] Richard J-M 2004 Safe domain and elementary geometry *Eur. J. Phys.* **25** 835–44
[14] Griffiths D J and Heald M A 1991 Time-dependent generalizations of the Biot–Savart and Coulomb laws *Am. J. Phys.* **59** 111–7
[15] Singal A K 2011 A first principles derivation of the electromagnetic fields of a point charge in arbitrary motion *Am. J. Phys.* **79** 1036–41
[16] Janah A R, Padmanabhan T and Singh T P 1988 On Feynman's formula for the electromagnetic field of an arbitrarily moving charge *Am. J. Phys.* **56** 1036–8
[17] Jefimenko O D 1994 Direct calculation of the electric and magnetic fields of an electric point charge moving with constant velocity *Am. J. Phys.* **62** 79–85
[18] Le Bellac M and Lévy-Leblond J M 1973 *Nuovo Cimento* B **14** 217–34
[19] de Montigny M and Rousseaux G 2006 On the electrodynamics of moving bodies at low velocities *Eur. J. Phys.* **27** 755–68
[20] Manfredi G 2013 Non-relativistic limits of Maxwell's equations *Eur. J. Phys.* **34** 859–71
[21] Nelson R A 1987 Generalized Lorentz transformation for an accelerated, rotating frame of reference *J. Math. Phys.* **28** 2379–83